Dynamic response of laminated and sandwich composite structures via 1D models based on Chebyshev polynomials

JOURNAL OF SANDWICH STRUCTURES & MATERIALS

Original Article

Journal of Sandwich Structures and Materials
2019, Vol. 21(4) 1428–1444

DOI: 10.1177/1099636217715582
journals.sagepub.com/home/jsm
SAGE

Dynamic response of laminated and sandwich composite structures via 1D models based on Chebyshev polynomials

A Pagani, M Petrolo and E Carrera

Abstract

This article presents the dynamic response of composite structures via refined beam models. The mode superposition method was used, and the Carrera Unified Formulation was exploited to create the advanced structural models. The finite element method was employed to compute the natural frequencies and modes. The main novelty of this article concerns the use of Chebyshev polynomials to define the displacement field above the cross-section of the beam. In particular, polynomials of the second kind were adopted, and the results were compared with those from analytical solutions and already established Carrera Unified Formulation-based beam models, which utilize Taylor and Lagrange polynomials to develop refined kinematics theories. Sandwich beams and laminated, thin-walled box beams were considered. Non-classical effects such as the cross-section distortion and bending/torsion coupling were evaluated. The results confirm the validity of the Carrera Unified Formulation for the implementation of refined structural models with any expansion functions and orders. In particular, the Chebyshev polynomials provide accuracies very similar to those from Taylor models. The use of high-order expansions, e.g. seventh-order, leads to results as accurate as those of Lagrange models which, from previous publications, are known as the most accurate Carrera Unified Formulation 1D models for this type of structural problems.

Keywords

Refined beam theories, finite elements, Carrera Unified Formulation, dynamic response, mode superposition

MUL_2 Group, Department of Mechanical and Aerospace Engineering, Politecnico di Torino, Torino, Italy

Corresponding author:
E Carrera, MUL_2 Group, Department of Mechanical and Aerospace Engineering, Politecnico di Torino, Corso Duca degli Abruzzi 24, 10129 Torino, Italy.
Email: erasmo.carrera@polito.it

Introduction

The development of one-dimensional (1D) structural models is of great interest to reduce the computational costs in many engineering applications. Advanced 1D models are required to have results as accurate as those of plate/shell (2D) and solid (3D) models. The Euler–Bernoulli Beam Theory (EBBT) [1] and the Timoshenko Beam Theory (TBT) [2,3] are the classical beam theories. The TBT enhances EBBT assuming constant shear strains across the cross-section. Slender and moderately thick, solid-section beams subjected to bending can be analyzed with good accuracy using these theories. In the last decades, many refined beam theories have been proposed to improve classical models, but preserving their computational efficiency. Some of the most important are discussed here, with particular attention paid to structural dynamics and composite structures. More comprehensive reviews can be found in [4,5].

The adoption of shear correction factors [6,7] is a common way to improve classical theories, although correction factors are strongly problem dependent. Another approach exploits refined displacement field above the cross-section of the beam to include non-classical effects such as warping and cross-section distortions. Typical examples are those in [8–19].

This article exploits refined beam models developed in the framework of the Carrera Unified Formulation (CUF). The CUF was initially developed for plates and shells [20,21], and then extended to beams [22,23]. In the CUF framework, refined structural models are built using expansions of the unknown variables. The number of terms of the expansion, i.e. the number of unknowns, can be chosen via a convergence analysis. The CUF has the great advantage to enable the implementation of any order structural models with no need of formal changes in the problem equations and matrices. Recently, the CUF 1D models have been used for structural dynamics; in particular, free-vibration [24–27] and dynamic response of thin-walled structures [28]. In the works above, higher order beam theories were obtained using Taylor-like Expansion (TE). Lagrange expansions (LE) and the component-wise approach were used in [29–33]. In [34], trigonometric, exponential and zig-zag models were used, whereas a beam theory based on Chebyshev Expansion (CE) polynomials has been introduced in [35]. CE models were then used for the dynamic response of typical aerospace structures in [36].

In the present work, the mode superposition method is combined with 1D CUF CE models to investigate the dynamic response of laminated structures. First, a simply supported beam subjected to a sinusoidal load is considered. Then, a sandwich structure subjected to harmonic loads and a composite box beam subjected to distributed loads are investigated. In this article, 'Higher order, hierarchical models by CUF' section presents an overview of the higher order beam theories developed in the framework of CUF. Moreover, the FEM approach and mode superposition method are briefly outlined. 'Numerical results' section is devoted to the presentation of the results obtained using the proposed CUF, whereas conclusions are drawn in the final section.

Higher order, hierarchical models by CUF

Given a generic beam structure, the Cartesian coordinate system adopted is shown in Figure 1. The cross-section Ω and the beam axis y are orthogonal. Moreover, the beam axis has boundaries $0 \leq y \leq L$. The validity of the formulation adopted is not affected by the shape of the cross-section, since the reported rectangular cross-section has merely explicative purposes. The displacement field of a beam model in the framework of CUF can be written in a compact form as follows:

$$\boldsymbol{u}(x, y, z, t) = F_\tau(x, z)\boldsymbol{u}_\tau(y, t), \quad \tau = 1, 2, \ldots, M \tag{1}$$

where $\boldsymbol{u} = \{u_x, u_y, u_z\}^T$ is the displacement vector; F_τ indicates the functions of the cross-section coordinates x and z; $\boldsymbol{u}_\tau$ is the generalized displacement vector; M indicates the number of terms in the expansion. The choice of F_τ and M is arbitrary. Thus, the basis functions adopted to model the displacement field across the section can be different and expanded to any order.

Considering TE polynomials as F_τ functions, one can obtain the models referred to as TE. For instance, the displacement field of a second-order TE model (TE2) can be expressed as follows:

$$\begin{aligned}
u_x(x, y, z, t) &= u_{x1}(y, t) + x\, u_{x2}(y, t) + z\, u_{x3}(y, t) + x^2\, u_{x4}(y, t) + xz\, u_{x5}(y, t) + z^2\, u_{x6}(y, t) \\
u_y(x, y, z, t) &= u_{y1}(y, t) + x\, u_{y2}(y, t) + z\, u_{y3}(y, t) + x^2\, u_{y4}(y, t) + xz\, u_{y5}(y, t) + z^2\, u_{y6}(y, t) \\
u_z(x, y, z, t) &= u_{z1}(y, t) + x\, u_{z2}(y, t) + z\, u_{z3}(y, t) + x^2\, u_{z4}(y, t) + xz\, u_{z5}(y, t) + z^2\, u_{z6}(y, t)
\end{aligned} \tag{2}$$

where $u_{x_1}, u_{y_1}, u_{z_1}, \ldots, u_{z_6}$ represent the components of the generalized displacement vector, i.e. the unknown variables. The classical models – EBBT and TBT – can be obtained as particular cases of the TE1.

Another class of CUF models is based on LE. In this work, mainly bi-quadratic nine-node (L9) Lagrange polynomials are used as F_τ. Lagrange polynomials can be found in [23]. The displacement field within an L9 element can be written as:

$$\begin{aligned}
u_x(x, y, z) &= F_1(x, z)u_{x1}(y) + F_2(x, z)u_{x2}(y) + \cdots + F_9(x, z)u_{x9}(y) \\
u_y(x, y, z) &= F_1(x, z)u_{y1}(y) + F_2(x, z)u_{y2}(y) + \cdots + F_9(x, z)u_{y9}(y) \\
u_z(x, y, z) &= F_1(x, z)u_{z1}(y) + F_2(x, z)u_{z2}(y) + \cdots + F_9(x, z)u_{z9}(y)
\end{aligned} \tag{3}$$

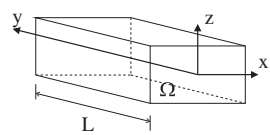

Figure 1. Coordinate frame of the beam.

The time variable t is omitted in the following for the sake of clarity. $u_{x1}, \ldots, u_{z9}$ are the translational components of the nine points of the L9 element. L-elements can be assembled above the cross-section imposing the displacement continuity at the interface nodes.

In this article, the CE is used for the first time to investigate the dynamic response of composite structures. For instance, the CE second-order kinematic model (CE2) has 18 generalized displacement variables, and can be defined as follows:

$$\begin{aligned} u_x(x,y,z) &= P_{00}(x,z)u_{x1}(y) + P_{10}(x,z)u_{x2}(y) + P_{01}(x,z)u_{x3}(y) \\ &\quad + P_{20}(x,z)u_{x4}(y) + P_{11}(x,z)u_{x5}(y) + P_{02}(x,z)u_{x6}(y) \\ u_y(x,y,z) &= P_{00}(x,z)u_{y1}(y) + P_{10}(x,z)u_{y2}(y) + P_{01}(x,z)u_{y3}(y) \\ &\quad + P_{20}(x,z)u_{y4}(y) + P_{11}(x,z)u_{y5}(y) + P_{02}(x,z)u_{y6}(y) \\ u_z(x,y,z) &= P_{00}(x,z)u_{z1}(y) + P_{10}(x,z)u_{z2}(y) + P_{01}(x,z)u_{z3}(y) \\ &\quad + P_{20}(x,z)u_{z4}(y) + P_{11}(x,z)u_{z5}(y) + P_{02}(x,z)u_{z6}(y) \end{aligned} \tag{4}$$

where $P_{00}, \ldots, P_{02}$ are the Chebyshev polynomials of the second kind, as shown in [35].

Finite element formulation

The stress $\boldsymbol{\sigma}$ and the strain $\boldsymbol{\epsilon}$ vectors are defined as follows:

$$\begin{aligned} \boldsymbol{\sigma} &= \left\{\sigma_{yy}, \sigma_{xx}, \sigma_{zz}, \sigma_{xz}, \sigma_{yz}, \sigma_{xy}\right\}^T \\ \boldsymbol{\epsilon} &= \left\{\epsilon_{yy}, \epsilon_{xx}, \epsilon_{zz}\epsilon_{xz}, \epsilon_{yz}, \epsilon_{xy}\right\}^T \end{aligned} \tag{5}$$

Under the assumption of small displacements and elongations, the following relation between strains and displacements holds:

$$\boldsymbol{\epsilon} = \boldsymbol{D}\boldsymbol{u} \tag{6}$$

$\boldsymbol{D}$ is the linear differential operator, defined as follows:

$$\boldsymbol{D} = \begin{bmatrix} 0 & \frac{\partial}{\partial y} & 0 \\ \frac{\partial}{\partial x} & 0 & 0 \\ 0 & 0 & \frac{\partial}{\partial z} \\ \frac{\partial}{\partial z} & 0 & \frac{\partial}{\partial x} \\ 0 & \frac{\partial}{\partial z} & \frac{\partial}{\partial y} \\ \frac{\partial}{\partial y} & \frac{\partial}{\partial x} & 0 \end{bmatrix} \tag{7}$$

Applying the constitutive law, one can obtain the stress components:

$$\boldsymbol{\sigma} = \tilde{\boldsymbol{C}}\boldsymbol{\epsilon} \tag{8}$$

For the sake of brevity, the explicit form of the coefficients $\tilde{\boldsymbol{C}}_{ij}$ in the previous relation is omitted. More details can be found in [37].

The shape functions N_i are used to interpolate the generalized displacement vector $\boldsymbol{u}_\tau$ along the y direction,

$$\boldsymbol{u}(x, y, z) = F_\tau(x, z)N_i(y)\boldsymbol{u}_{\tau i} \tag{9}$$

where $\boldsymbol{u}_{\tau i}$ is the nodal unknown vector. In the present work, four-node (B4) 1D elements have been used; this leads to a cubic approximation along the y axis. The internal strain energy L_{int} can be related to the work of the inertial loads L_{ine} according to the principle of virtual displacements:

$$\delta L_{int} = \int_V \delta\boldsymbol{\epsilon}^T\boldsymbol{\sigma}\,\mathrm{d}V = -\delta L_{ine} \tag{10}$$

where δ stands for virtual variation. The virtual variation of the strain energy can be written in a compact form combining equations (6), (8) and (9):

$$\delta L_{int} = \delta\boldsymbol{u}_{sj}^T\boldsymbol{K}^{ij\tau s}\boldsymbol{u}_{\tau i} \tag{11}$$

In the above relation, the fundamental nucleus of the stiffness matrix is $\boldsymbol{K}^{ij\tau s}$, whereas the four indexes indicated by the superscripts are those used to expand the elemental matrix. In particular, i and j are related to the shape functions N_i and N_j, whereas τ and s are related to the expansion functions F_τ and F_s. The 3×3 array which represents the fundamental nucleus is formally independent of the order of the beam model. A more detailed explanation of the expansion of nuclei and assembly procedures in FEM framework can be found in [23]. The work of the inertial loadings can be written in terms of virtual variation,

$$\delta L_{ine} = \int_V \rho\delta\boldsymbol{u}^T\ddot{\boldsymbol{u}}\,\mathrm{d}V \tag{12}$$

In the above equation, ρ stands for the density of the material, whereas $\ddot{\boldsymbol{u}}$ is the acceleration vector. By substituting equation (9) into equation (12), one has

$$\delta L_{ine} = -\delta\boldsymbol{u}_{sj}^T\int_L N_iN_j\mathrm{d}y\int_\Omega \rho F_\tau F_s d\Omega\ddot{\boldsymbol{u}}_{\tau i} = -\delta\boldsymbol{u}_{sj}^T\boldsymbol{M}^{ij\tau s}\ddot{\boldsymbol{u}}_{\tau i} \tag{13}$$

where $\boldsymbol{M}^{ij\tau s}$ is the fundamental nucleus of the elemental mass matrix and $\ddot{\boldsymbol{u}}_{\tau i}$ indicates the nodal acceleration vector. The components of the elemental mass are:

$$\begin{aligned} \boldsymbol{M}_{xx}^{ij\tau s} = \boldsymbol{M}_{yy}^{ij\tau s} = \boldsymbol{M}_{zz}^{ij\tau s} = \int_L N_i N_j \mathrm{d}y \int_\Omega \rho F_\tau F_s \mathrm{d}\Omega \\ \boldsymbol{M}_{xy}^{ij\tau s} = \boldsymbol{M}_{xz}^{ij\tau s} = \boldsymbol{M}_{yx}^{ij\tau s} = \boldsymbol{M}_{zx}^{ij\tau s} = \boldsymbol{M}_{yz}^{ij\tau s} = \boldsymbol{M}_{zy}^{ij\tau s} = 0 \end{aligned} \tag{14}$$

It should be noted that no assumptions have been made on the expansion order of the theory, even in the case of the inertial terms. In fact, using this formulation, several refined beam models can be developed without any formal change in the fundamental nucleus components.

The fundamental nuclei are substituted into the principle of virtual displacement (equation (10)) to obtain the undamped dynamic problem. The CUF fundamental nuclei are then expanded, and the global FEM arrays are assembled,

$$\boldsymbol{M}\ddot{\boldsymbol{u}} + \boldsymbol{K}\boldsymbol{u} = 0 \tag{15}$$

The second-order system of ordinary differential equations is reduced into a classical eigenvalue problem if harmonic solutions are considered,

$$\left(-\omega_k^2 \boldsymbol{M} + \boldsymbol{K}\right)\boldsymbol{u}_k = 0 \tag{16}$$

where $\boldsymbol{u}_k$ is the k-th eigenvector.

Mode superposition method

The equilibrium governing equations of the dynamic response in a system with multiple degrees of freedom (DOFs) are [38]:

$$\boldsymbol{M}\ddot{\boldsymbol{u}}(t) + \boldsymbol{C}\dot{\boldsymbol{u}}(t) + \boldsymbol{K}\boldsymbol{u}(t) = \boldsymbol{P}(t) \tag{17}$$

where $\boldsymbol{C}$ is the damping matrix and $\boldsymbol{P}$ is the time-dependant loading vector, which is computed in the framework of CUF as in [23]. The vector of unknowns $\boldsymbol{u}$ is transformed in accordance with the superposition method:

$$\boldsymbol{u}(t) = \Phi \boldsymbol{x}(t) \tag{18}$$

where Φ is a $DOFs \times m$ matrix containing m $\boldsymbol{M}$-orthonormalized eigenvectors and $\boldsymbol{x}(t)$ is a time-dependent vector of order m. To transform the equations of motion, each term of equation (18) is substituted into the governing equations (equation (17)) and pre-multiplied by Φ^T

$$\ddot{\boldsymbol{x}}(t) + \Phi^T \boldsymbol{C} \Phi\, \dot{\boldsymbol{x}}(t) + \Omega^2 \boldsymbol{x}(t) = \Phi^T \boldsymbol{P}(t) \tag{19}$$

where Ω^2 is the diagonal matrix that stores the eigenvalues ω_i^2. If the damping is neglected, from equation (19), one can notice that the equations of motion are decoupled. Hence, m individual equations can be obtained by decomposing this relation. The solution for each equation is computed by means of the Duhamel integral

$$\left.\begin{aligned} \ddot{x}_i(t) + \omega_i^2 x_i(t) &= r_i(t) \\ r_i(t) &= \Phi_i \boldsymbol{P}(t) \end{aligned}\right\} \quad i = 1, 2, \ldots, n \tag{20}$$

$$x_i(t) = \frac{1}{\omega_i} \int_0^t r_i(\tau) \sin \omega_i (t - \tau) \mathrm{d}\tau + \alpha_i \sin \omega_i t + \beta_i \cos \omega_i t \tag{21}$$

To compute α_i and β_i, initial conditions need to be addressed. The contribution to the response for each mode is obtained after the solution for each of the m equations is calculated.

$$\boldsymbol{u}^m(t) = \sum_{i=1}^{m} \Phi_i x_i(t) \tag{22}$$

In this approach, the accuracy of the solution depends on m.

Numerical results

This section presents the numerical results of this article. First, preliminary analyses were carried out on an isotropic structure. Then, a sandwich beam and a laminated box beam were considered.

Compact square section

A first, preliminary assessment is presented in this section to validate the modal superposition methodology. A simply supported, square section beam is considered. The cross-section height is 0.1 m, the span-to-height ratio L/h is 100, and the material properties are $E = 69\,\mathrm{GPa}$, $v = 0.33$ and $\rho = 2700\ \frac{\mathrm{kg}}{\mathrm{m}^3}$. A vertical, harmonic force was applied at the centre of the mid-span section, $P_z(t) = P_{z0} \sin(\omega t)$, where $P_{z0} = -1000\,\mathrm{N}$ is the amplitude of the sinusoidal load, and $\omega = 7\ \frac{\mathrm{rad}}{\mathrm{s}}$ is the angular frequency. According to the Euler–Bernoulli beam assumptions, the peak response can be approximated as follows [38]:

$$u_{z_{max}DYN} \simeq \frac{2P_{z0}L^3}{\pi^4 EI} \frac{1}{1 - \frac{\omega}{\omega_1}} \tag{23}$$

where I is the moment of inertia of the beam cross-section. Such an approximation is valid as soon as $\omega_1 > \omega$, in which ω_1 is the bending, first fundamental angular

frequency. The dynamic response was investigated using the modal superposition and the present CUF models over the time interval [0, 8] s. Table 1 shows the maximum transverse displacements at the centre of the mid-space cross-section. In particular, this table compares the approximated analytical value, TE and CE models up to the third-order. Figure 2 shows the loading point transverse displacement over the time interval using the analytical solution based on Euler–Bernoulli and CE3. There is a good match between the analytical results and those from the finite element models. The use of refined models does not modify the solution to a great extent. As well known, slender, homogenous beams under bending are well

Table 1. Maximum transverse displacement (mm) using different theories, square beam.

Model	$u_{z_{max}DYN}$	ω_1
Analytical	–69.4719	14.4030
*TE*3	–70.0014	14.4006
*CE*3	–70.0019	14.3999

TE: Taylor-like Expansion; CE: Chebyshev Expansion.

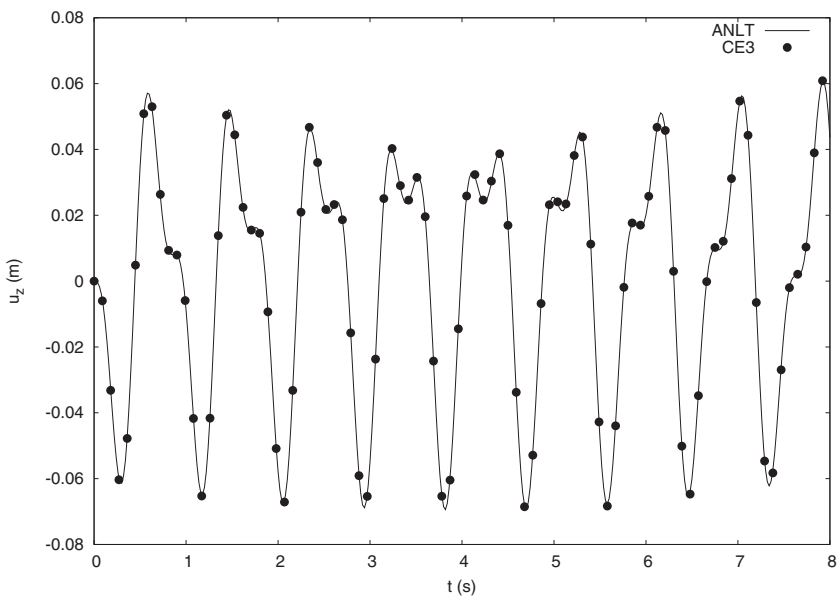

Figure 2. Transverse displacement at the centre of the mid-span section for different models, square beam.

modelled by classical theories. The results from CE models match perfectly the TE ones.

Sandwich beam

This section presents the dynamic response of a clamped–clamped sandwich beam. The free vibration analysis of this beam was presented in [39]. The structure consists of two face sheets (*f*) bonded to a core (*c*). Isotropic materials were employed with $E_f = 68.9$ GPa, $E_c = 179.014$ MPa, $G_f = 26.5$ GPa, $G_c = 68.9$ MPa, $\rho_f = 2687.3\,\mathrm{kg/m^3}$ and $\rho_c = 119.69\,\mathrm{kg/m^3}$. Figure 3 shows the cross-section geometry, with $h_f = 0.40624$ mm, $h_c = 6.3475$ mm, $b = 25.4$ mm and $L = 1.2187$ m. Two different loading cases were considered, as shown in Figure 3. Both load cases have a sinusoidal load having amplitude $F_0 = -10$ N and angular frequency $\omega = 30$ rad/s.

The time-dependent transverse displacement at the mid-span load application point is shown in Figure 4 for various theories, whereas the maximum and minimum displacements are reported in Table 2. The maximum deformation of the cross-section at mid-span is reported in Figure 5 for Case 1. The results suggest that

- Overall, classical models can detect the time-dependent displacement behaviour of the structures. However, significant differences were found in the maximum values due to the neglecting of torsion and the in-plane distortion of the cross-section.
- The novel CE models are as accurate as TE models and in good agreement with LE.

Six-layer composite box beam

A cantilever, thin walled, hollow, rectangular beam was considered. This structure has been previously investigated in [40–43] in which free vibration analyses were carried out. The structure consists of a six-layer laminated box beam with hollow rectangular cross-section, whose dimensions are length $L = 844.55$ mm, height $h = 13.6$ mm, width $b = 24.2$ mm and thickness $t = 0.762$ mm. Each layer has the

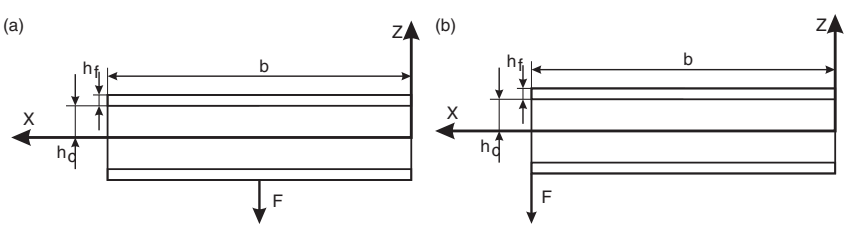

Figure 3. Cross-section geometry of the sandwich beam and application points of the sinusoidal loads. (a) Case I and (b) Case II.

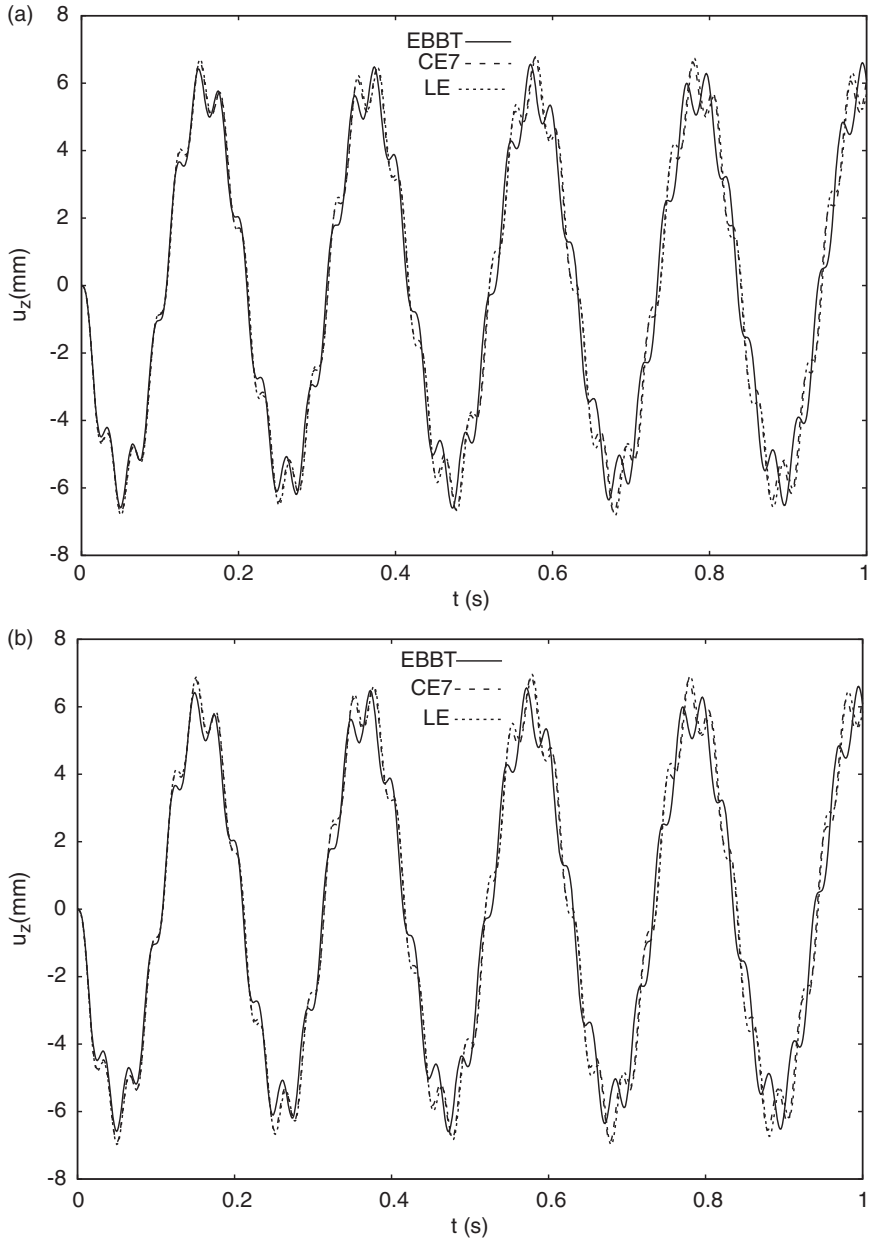

Figure 4. Transverse displacement at the mid-span load application point for various theories, sandwich beam model. (a) Case I and (b) Case II.

Table 2. Maximum and minimum transverse displacement (mm) at the mid-span cross-section obtained by means of various theories, sandwich beam.

		Case I		Case II	
Theory	DOFs	$u_{z_{max}}$	$u_{z_{min}}$	$u_{z_{max}}$	$u_{z_{min}}$
EBBT	93	6.612	–6.600	6.604	–6.596
TBT	155	6.612	–6.600	6.612	–6.600
*TE*2	558	6.472	–6.517	6.476	–6.521
*TE*7	3348	6.751	–6.742	6.916	–6.907
*CE*2	558	6.472	–6.517	6.476	–6.521
*CE*7	3348	6.751	–6.743	6.917	–6.908
LE	7533	6.795	–6.819	6.958	–6.982

EBBT: Euler–Bernoulli Beam Theory; TBT: Timoshenko Beam Theory; TE: Taylor-like Expansion; CE: Chebyshev Expansion; LE: Lagrange expansion.

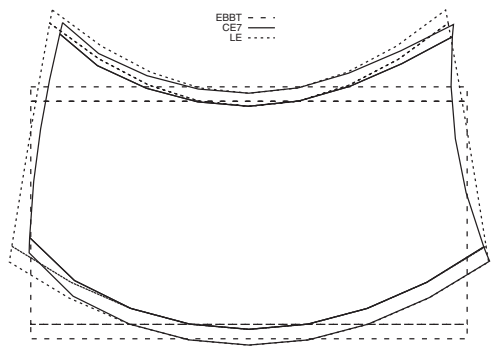

Figure 5. Deformation of the mid-span cross-section of the sandwich beam, Case I.

same thickness. Two material cases were considered. The same aluminium alloy of the previous case was employed for the isotropic case. Moreover, an orthotropic material having the following properties was considered,

$$E_1 = 141.96\,\text{GPa} \quad E_2 = E_3 = 9.79\,\text{GPa} \quad \nu_{12} = \nu_{13} = 0.42 \quad \nu_{23} = 0.5$$
$$G_{12} = G_{13} = 6.0\,\text{GPa} \quad G_{23} = 4.83\,\text{GPa} \quad \rho = 1445.0\,\frac{\text{kg}}{\text{m}^3}$$

Different stacking sequences and ply angles were taken into account, namely the circumferentially asymmetric stiffness (CAS) and circumferentially uniform stiffness (CUS), as in Table 3. The box beam was subjected to a pressure load whose distribution across the section is shown in Figure 6. The load was uniformly distributed in the span-wise direction while a linear distribution was considered along the width. The distributed load resultant is 10 N, whereas the height of the linear

Table 3. Stacking sequences of the six-layer box beam.

	Flanges		Webs	
Layup	Top	Bottom	Left	Right
*CAS*2	$[30]_6$	$[30]_6$	$[30/-30]_3$	$[30/-30]_3$
*CAS*3	$[45]_6$	$[45]_6$	$[45/-45]_3$	$[45/-45]_3$
*CUS*1	$[15]_6$	$[-15]_6$	$[15]_6$	$[-15]_6$
*CUS*2	$[0/30]_3$	$[0/-30]_3$	$[0/30]_3$	$[0/-30]_3$
*CUS*3	$[0/45]_3$	$[0/-45]_3$	$[0/45]_3$	$[0/-45]_3$

CAS: circumferentially asymmetric stiffness; CUS: circumferentially uniform stiffness.

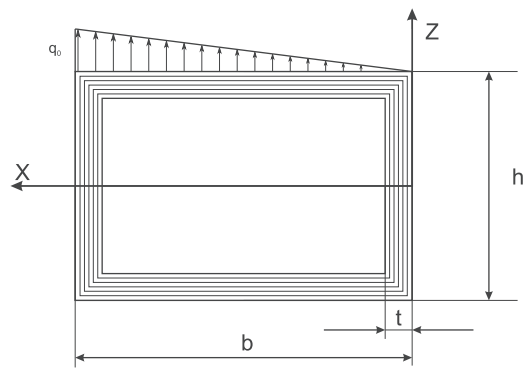

Figure 6. Load distribution for the box beam.

Table 4. Maximum transverse displacement (mm) at the free tip of the six-layer box beam using various models.

Model	*TE*3	*TE*7	*CE*3	*CE*7	LE
DOFs	930	3348	930	3348	19344
CAS2	14.085	15.000	14.087	14.992	15.247
CAS3	33.842	37.012	33.845	36.948	37.517
CUS1	8.056	8.923	8.057	8.923	9.190
CUS2	5.581	5.755	5.582	5.756	5.770
CUS3	6.529	6.590	6.529	6.591	6.560
Isotropic	3.447	3.453	3.447	3.453	3.454

TE: Taylor-like Expansion; CE: Chebyshev Expansion; LE: Lagrange expansion; DOFs: degrees of freedom; CAS: circumferentially asymmetric stiffness; CUS: circumferentially uniform stiffness.

distribution is 10/L N/m. The load was modelled as a function of the time according to the following relation:

$$q = \begin{cases} \frac{q_0}{t_1}, & t \in [0, t_1] \\ q_0, & t > t_1 \end{cases} \tag{24}$$

The analysis was performed considering $t_1 = 0.05$ s. Table 4 shows the transverse displacement for various models, whereas Figure 7 shows the transverse

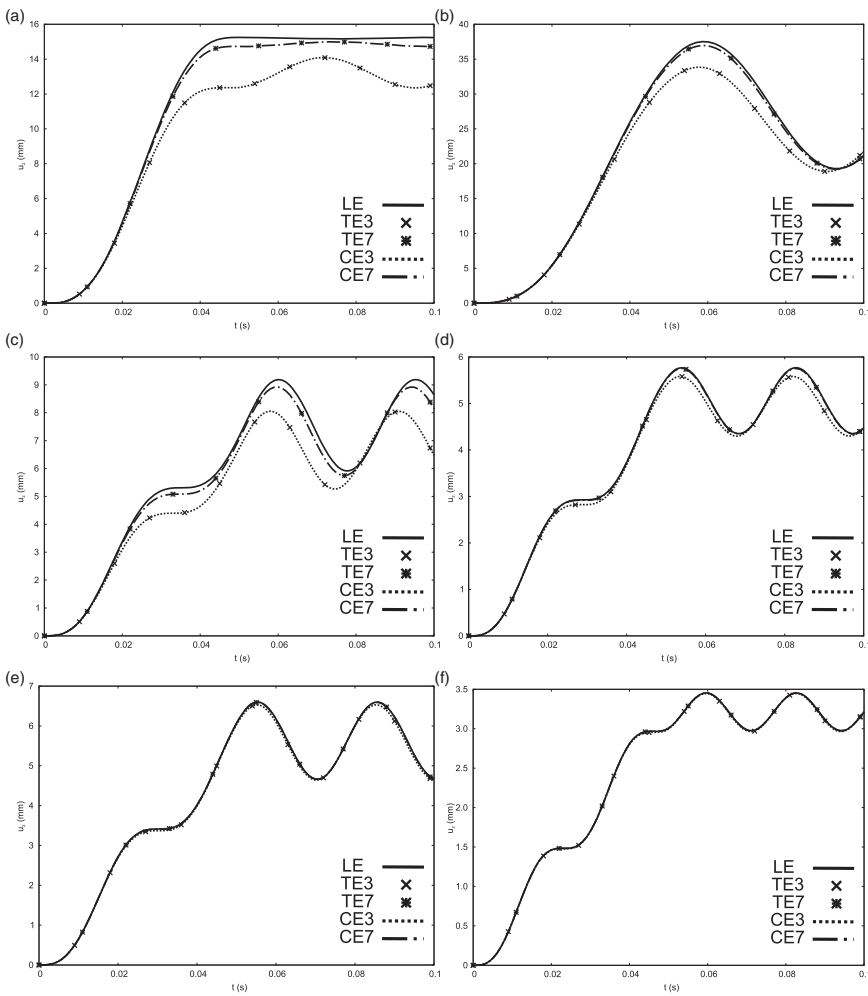

Figure 7. Time-dependent transverse displacement at the free tip of the six-layer box beam for various theories. (a) CAS2, (b) CAS3, (c) CUS1, (d) CUS2, (e) CUS3, and (f) isotropic. CAS: circumferentially asymmetric stiffness; CUS: circumferentially uniform stiffness.

displacement over the time interval considered. Figure 8 shows the distortion of the free tip cross-section via CE7 and LE. The results suggest that

- Perfect agreement was found between CE and TE.
- Depending on the stacking sequence, different expansion orders are needed to detect accurate results. In particular, CAS2, CAS3 and CUS1 may require

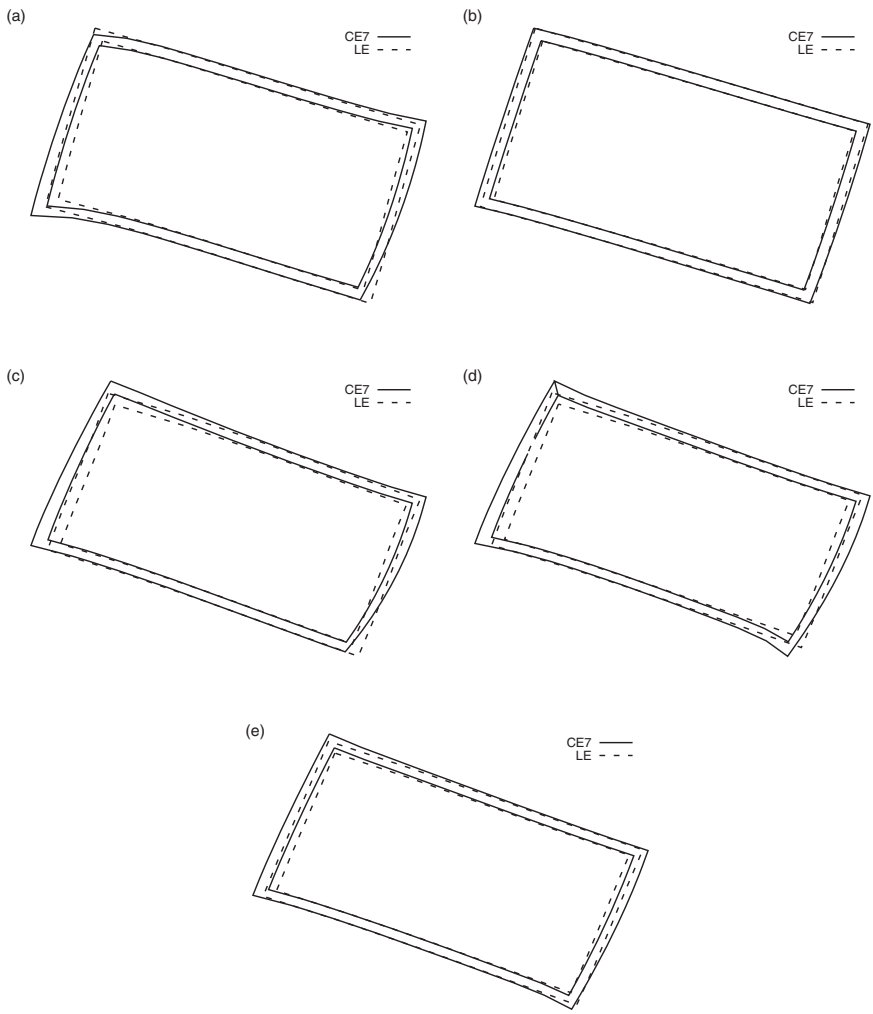

Figure 8. Free tip cross-section distortion, six-layer composite box beam. (a) CAS2, $t = 0.049$ s; (b) CAS3, $t = 0.059$ s; (c) CUS1, $t = 0.059$ s; (d) CUS2, $t = 0.054$ s; (e) CUS3, $t = 0.055$ s. CAS: circumferentially asymmetric stiffness; CUS: circumferentially uniform stiffness.

seventh or higher orders while, in the other cases, third-order models are enough. Similar results were found for the free vibration analysis [35].
- The distortion of the cross-section from CE models matches LE with good accuracy.

Conclusions

This article has dealt with the dynamic response of laminated and sandwich structures. 1D CUF refined structural models have been employed together with the finite element method and the mode superposition method. In particular, the Chebyshev polynomial expansions have been used to model the displacement field above the cross-section of the structure. The main aim of this article has been the investigation of the accuracy of the Chebyshev-based 1D models for structural dynamics problems of composite structures. Numerical assessments have dealt with compact homogeneous and sandwich beams as well as a six-layer box structure. The results have been compared with those from Taylor and Lagrange 1D models and analytical solutions. The results suggest that

- The novel CE models have proved to be as accurate as Taylor models (TE). In most cases, seventh-order expansions can match the accuracy of Lagrange models (LE). However, TE and CE models usually require fewer DOFs than LE.
- Higher order expansions can detect torsion, bending/torsion coupling and cross-section distortions properly.
- As a general guideline, TE and CE should be used when global non-local effects have to be investigated. On the other hand, LE should be preferred to deal with local effects.

Declaration of Conflicting Interests

The author(s) declared no potential conflicts of interest with respect to the research, authorship, and/or publication of this article.

Funding

The author(s) disclosed receipt of the following financial support for the research, authorship, and/or publication of this article: Erasmo Carrera has been partially supported by the Russian Science Foundation (Grant No. 15-19-30002).

References

1. Euler L. *De curvis elasticis*. Geneva: Bousquet, 1744.
2. Timoshenko S. On the corrections for shear of the differential equation for transverse vibration of prismatic bars. *Philos Mag* 1922; 41: 744–746.
3. Timoshenko S. On the transverse vibrations of bars of uniform cross section. *Philos Mag* 1922; 41: 122–131.

4. Kapania RK and Raciti S. Recent advances in analysis of laminated beams and plates, part II: Vibrations and wave propagation. *AIAA J* 1989; 27: 935–946.
5. Carrera E, Pagani A, Petrolo M, et al. Recent developments on refined theories for beams with applications. *Mech Eng Rev* 2015; 2: 14–00298–14–00298.
6. Timoshenko S and Goodier J. *Theory of elasticity*. New York: McGraw-Hill, 1970.
7. Dong S, Alpdogan C and Taciroglu E. Much ado about shear correction factors in Timoshenko beam theory. *Int J Solids Struct* 2010; 47: 1651–1665.
8. Heyliger P and Reddy J. A higher order beam finite element for bending and vibration problems. *J Sound Vib* 1988; 126: 309–326.
9. Kant T and Gupta A. A finite element model for a higher-order shear-deformable beam theory. *J Sound Vib* 1988; 125: 193–202.
10. Marur S and Kant T. Free vibration analysis of fiber reinforced composite beams using higher order theories and finite element modelling. *J Sound Vib* 1996; 194: 337–351.
11. Marur S and Kant T. On the angle ply higher order beam vibrations. *Comput Mech* 2007; 40: 25–33.
12. Kant T, Marur S and Rao G. Analytical solution to the dynamic analysis of laminated beams using higher order refined theory. *Compos Struct* 1997; 40: 1–9.
13. Marur S and Kant T. On the performance of higher order theories for transient dynamic analysis of sandwich and composite beams. *Comput Struct* 1997; 65: 741–759.
14. Librescu L and Na S. Boundary control of free and forced oscillation of shearable thin-walled beam cantilevers. *Eur J Mech A/Solids* 1998; 17: 687–700.
15. Librescu L and Na S. Dynamic response of cantilevered thin-walled beams to blast and sonic-boom loadings. *Shock Vib* 1998; 5: 23–33.
16. Soldatos K and Elishakoff I. A transverse shear and normal deformable orthotropic beam theory. *J Sound Vib* 1992; 155: 528–533.
17. Subramanian P. Dynamic analysis of laminated composite beams using higher order theories and finite elements. *Compos Struct* 2006; 73: 342–353.
18. Ganesan R and Zabihollah A. Vibration analysis of tapered composite beams using a higher-order finite element. Part I: Formulation. *Compos Struct* 2007; 77: 306–318.
19. Orzechowski G and Shabana A. Analysis of warping deformation modes using higher order ANCF beam element. *J Sound Vib* 2016; 363: 428–445.
20. Carrera E. Theories and finite elements for multilayered, anisotropic, composite plates and shells. *Archiv Comput Methods Eng* 2002; 9: 87–140.
21. Carrera E. Theories and finite elements for multilayered plates and shells: a unified compact formulation with numerical assessment and benchmarking. *Archiv Comput Methods Eng* 2003; 10: 216–296.
22. Carrera E, Giunta G and Petrolo M. *Beam structures classical and advanced theories*. Chichester, UK: John Wiley & Sons, Ltd, 2011.
23. Carrera E, Cinefra M, Petrolo M, et al. *Finite element analysis of structures through unified formulation*. Chichester, UK: John Wiley & Sons Ltd, 2014.
24. Carrera E, Petrolo M and Varello A. Advanced beam formulations for free vibration analysis of conventional and joined wings. *J Aerosp Eng* 2012; 25: 282–293.
25. Petrolo M, Zappino E and Carrera E. Unified higher-order formulation for the free vibration analysis of one-dimensional structures with compact and bridge-like cross-sections. *Thin Wall Struct* 2012; 56: 49–61.

26. Pagani A, Boscolo M, Banerjee JR, et al. Exact dynamic stiffness elements based on one-dimensional higher-order theories for free vibration analysis of solid and thin-walled structures. *J Sound Vib* 2013; 332: 6104–6127.
27. Dan M, Pagani A and Carrera E. Free vibration analysis of simply supported beams with solid and thin-walled cross-sections using higher-order theories based on displacement variables. *Thin Wall Struct* 2016; 98(Part B): 478–495.
28. Carrera E and Varello A. Dynamic response of thin-walled structures by variable kinematic one-dimensional models. *J Sound Vib* 2012; 331: 5268–5282.
29. Carrera E, Pagani A and Petrolo M. Component-wise method applied to vibration of wing structures. *J Appl Mech* 2013; 80: Article number 011006.
30. Carrera E and Pagani A. Free vibration analysis of civil engineering structures by component-wise models. *J Sound Vib* 2014; 333: 4597–4620.
31. Carrera E and Zappino E. Carrera Unified Formulation for free-vibration analysis of aircraft structures. *AIAA J* 2016; 54: 280–292.
32. Carrera E and Pagani A. Accurate response of wing structures to free-vibration, load factors, and nonstructural masses. *AIAA J* 2016; 54: 227–241.
33. Carrera E, Pagani A and Petrolo M. Free vibrations of damaged aircraft structures by component-wise analysis. *AIAA J* 2016; 54: 3091–3106.
34. Carrera E, Filippi M and Zappino E. Laminated beam analysis by polynomial, trigonometric, exponential and zig-zag theories. *Eur J Mech - A/Solids* 2013; 41: 58–69.
35. Filippi M, Pagani A, Petrolo M, et al. Static and free vibration analysis of laminated beams by refined theory based on Chebyshev polynomials. *Compos Struct* 2015; 132: 1248–1259.
36. Pagani A, Petrolo M, Colonna G, et al. Dynamic response of aerospace structures by means of refined beam theories. *Aerosp Sci Technol* 2015; 46: 360–373.
37. Reddy JN. *Mechanics of laminated composite plates and shells. Theory and analysis*, 2nd ed. Boca Raton: CRC Press, 2004.
38. Volterra E and Zachmanoglou E. *Dynamics of vibrations*. Ohio, USA: Charles E. Merill Books Inc., 1965.
39. Carrera E, Filippi M and Zappino E. Free vibration analysis of laminated beam by polynomial, trigonometric, exponential and zig-zag theories. *J Compos Mater* 2014; 48: 2299–2316.
40. Armanios E and Badir A. Free vibration analysis of anisotropic thin-walled closed-section beams. *AIAA J* 1995; 33: 1905–1910.
41. Gunay M and Timarci T. Free vibration of composite box-beams by Ansys. In: *International scientific conference (UNITECH)*, Gabrovo, Bulgaria, 16–17 November 2012.
42. Chandra R and Chopra I. Experimental-theoretical investigation of the vibration characteristics of rotating composite box beams. *J Aircraft* 1992; 29: 657–664.
43. Carrera E, Filippi M, Mahato P, et al. Advanced models for free vibration analysis of laminated beams with compact and thin-walled open/closed sections. *J Compos Mater* 2015; 49: 2085–2101.